Self-Field Effects in a Josephson Junction Model for J_c in REBCO Tapes

Charles W. A. Gurnham and Damian P. Hampshire

***Abstract*—We have modeled the effects of self-field on the critical current density J_c in high temperature superconducting REBCO tapes, by considering them as a collection of Josephson junctions (JJs) in parallel. We have used a 2D JJ framework for each junction and included their component self-field effects using the well known expression for the magnetic field produced by a thin strip. We provide computational and analytic expressions for the spatial distribution of J_c, enabling us to calculate the critical current of coated conductors over the whole field range. We find that J_c in self field for thin tapes is broadly independent of the width but strongly dependent on the thickness of the tape. For example, if a tape thickness is doubled, even if J_c is unchanged in high field, we expect the self-field J_c to drop by $\sim$ 20 % because of the larger self-field produced. Our results are compared to experimental results for technological coated conductors from the literature and good agreement is found.**

***Index Terms*—Critical current density, High-temperature superconductors, Josephson junctions, Superconducting thin films**

I. Introduction

THE current density in commercial high temperature superconducting tapes is now so high that the self-field of even single 4 mm wide tapes can be tens of mT at 77 K and an order of magnitude larger at low temperatures. This means that homogeneous tapes of different widths and thicknesses have different values of current density in self-field, which can be a concern when, for example, batch testing tapes of different geometry from different suppliers for use in magnets. Recent work in our group [1] has generalized the solutions found by Fink [2] in zero applied field for a very narrow and thick Josephson junction (JJ), to arbitrary applied field and shown using time-dependent Ginzburg-Landau simulations that these solutions have a wide range of validity [1]. In this paper we extend these solutions for J_c down to low magnetic fields, where there is the additional complexity that the transport current can produce a magnetic field that is comparable to, or larger than, the applied field. In particular we address how the width and thickness of the tape affects J_c in this low applied field regime.

Manuscript receipt and acceptance dates will be inserted here. This work was supported by the Engineering and Physical Sciences Research Council. EP/L01663X/1. *(Corresponding author: Charles Gurnham.)*

The authors are with the Superconductivity Group, Durham University, South Road, Durham, DH1 3LE, U.K. (e-mail: charles.gurnham@durham.ac.uk; d.p.hampshire@durham.ac.uk). Color versions of one or more of the figures in this paper are available online at http://ieeexplore.ieee.org.

The data are available at http://dx.doi.org/10.15128/r1d504rk36k and associated materials can be found at Durham Research Online: http://dro.dur.ac.uk/.

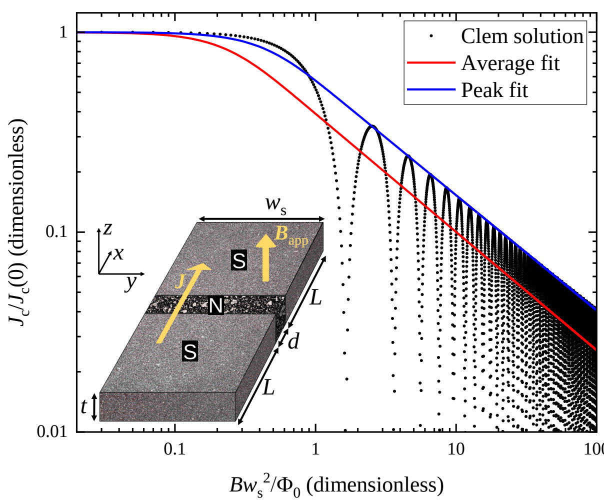

Fig. 1. Fit to Clem's solution [3] for the critical current density through a JJ as a function of magnetic field for superconducting electrodes with an aspect ratio of 1 (see (7)). Fits are shown both through the peaks and through field averaged data. Inset: JJ geometry, with square electrodes that have an aspect ratio of 1.

II. 2D Josephson Junctions in High Magnetic Fields

The expression derived [1] for narrow JJs of width w_s, with several fluxons in the junctions, in high magnetic fields up to B_{c2}, is of the form:

$$J_c(B,T) = C_0 \left(\frac{\phi_0}{Bw_s^2}\right)^{C_1} J_{DJ}(B,T), \tag{1}$$

where B is the magnetic field, T is the temperature, and C_0 and C_1 are constants. The first factor in (1) that includes C_0 and C_1 follows from the high field forms of J_c that include the sinc function for low aspect ratio superconducting electrodes in the JJ, and the Bessel function for the high aspect ratio electrodes, as derived by Clem [3]. The second factor $J_{DJ}(B,T)$ is essentially the depairing current density were the JJ to be very narrow. The terms in $J_{DJ}(B,T)$ are given by

$$J_{DJ}(B,T) = \frac{4J_0}{\tilde{s}\tilde{v}}(1-b)^{\frac{3}{2}}\left(1-\sqrt{1-\tilde{s}\tilde{f}^2_{\frac{d}{2}}}\right)\mathrm{e}^{-\frac{d}{\tilde{\xi}_n}}, \tag{2}$$

$$\tilde{v} = \frac{\tilde{m}_n\tilde{\xi}_n}{\tilde{\Upsilon}_n}\sqrt{1-b}, \qquad \tilde{s} = \frac{\tilde{\beta}_n(1-b)}{\left(\tilde{\alpha}_n - \frac{\tilde{\Upsilon}_n}{\tilde{m}_n}b\right)}, \tag{3}$$

$$\xi_{\mathrm{n}} = \sqrt{\frac{\tilde{\Upsilon}_{\mathrm{n}}}{\tilde{m}_{\mathrm{n}}\left(-\tilde{\alpha}_{\mathrm{n}} + \frac{\tilde{\Upsilon}_{\mathrm{n}}}{\tilde{m}_{\mathrm{n}}} b\right)}}\xi_{\mathrm{s}}, \qquad b = \frac{B}{B_{\mathrm{c2}}}, \tag{4}$$

and
$$\tilde{f}^2_{\frac{\mathrm{d}}{2}} = \frac{\tilde{v}^2 + 1 - \sqrt{\tilde{v}^2(2-\tilde{s})+1}}{\tilde{v}^2+\tilde{s}}, \tag{5}$$

where we have used the constraint $\tilde{\alpha}_{\mathrm{n}}(0) = -|T_{\mathrm{cn}}/T_{\mathrm{c}}|$. The temperature dependence of the Ginzburg-Landau parameter is taken from the Ginzburg-Landau ratio of the critical fields [4] using the standard temperature dependence for the upper critical field [5] and a two-fluid model for the critical field [6]. The temperature dependence of the coherence length is given by the Ginzburg-Landau relation for $B_{\mathrm{c2}}(T)$ [4]. J_0 is defined by

$$J_0 = \frac{B_{\mathrm{c2}}}{\mu_0 \kappa^2 \xi_{\mathrm{s}}}. \tag{6}$$

Thereafter the temperature dependence of the superconducting free parameters broadly follow text-book forms [4] and are provided elsewhere [1].

The most straightforward approach to the normal state properties of the junction has been adopted, where α_{n} has a linear temperature dependence above T_{cn} and β_{n} is a temperature independent constant. In our fits, we took the value of T_{c} to be 90 K and the values of B_{c2} at 77 K and 4.2 K to be 8 T and 115 T respectively. The free parameters are listed in Table I below - the form proposed enables us to describe both variable field and variable temperature J_{c} data [1]. We also note that the conclusions in this paper about the role of self-field are not sensitive to the precise details of the functional form used for $J_{\mathrm{DJ}}(B,T)$.

III. Josephson Junctions in Low Magnetic Fields

Here we replace the first factor in (1) with a form that ensures J_{c} remains finite even in zero field given by:

$$J_{\mathrm{c}}(B,T) = c_0 \left(\frac{\Phi_0 \tanh\frac{B}{B_0}}{B w_{\mathrm{s}}^2}\right)^{c_1} J_{\mathrm{DJ}}(B,T), \tag{7}$$

and more closely approaches the envelope of the sinc function and the Bessel function found in Clem's work [3]. Again, c_0 and c_1 are constants, and we have introduced the constraint

$$B_0 = \frac{\Phi_0}{w_{\mathrm{s}}^2} c_0^{\frac{1}{c_1}} \tag{8}$$

so that in the low-field limit $J_{\mathrm{c}} = J_{\mathrm{DJ}}(0,T)$. Capturing the low-field behaviour with (7) eliminates the singularities that occur at zero-field in (1) and avoids non-physical solutions. The parameters c_0 and c_1 are calculated by fitting (7) to Clem's low field numerical solutions for J_{c} through a JJ [3] as a function of the aspect ratio of the superconducting electrodes in the junction and shown in Fig. 1. We find $c_0 \approx c_1 \approx 0.6$ for an aspect ratio of 1.

As both c_0 and c_1 decrease monotonically with aspect ratio, we can describe the relation between the two using

$$c_1 = a_0 \cdot \ln(c_0) + a_1, \tag{9}$$

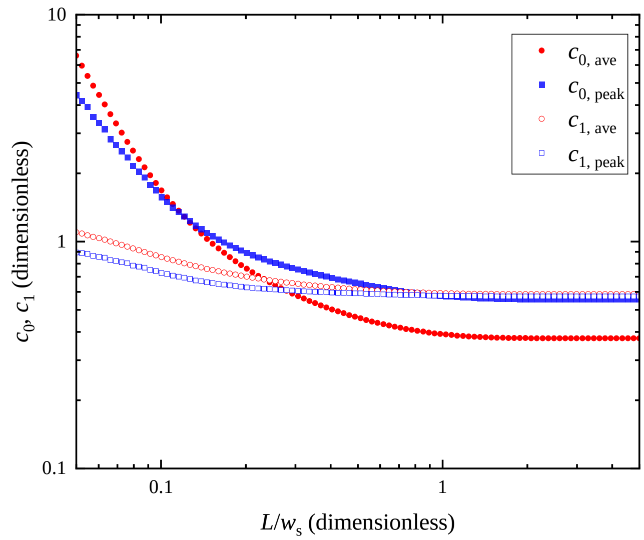

Fig. 2. The constants c_0 & c_1 derived from fits using (7) to Clem's expression for the critical current density through a JJ [3], as shown in Fig. 1, for JJs with electrodes of different aspect ratios L/w_{s}.

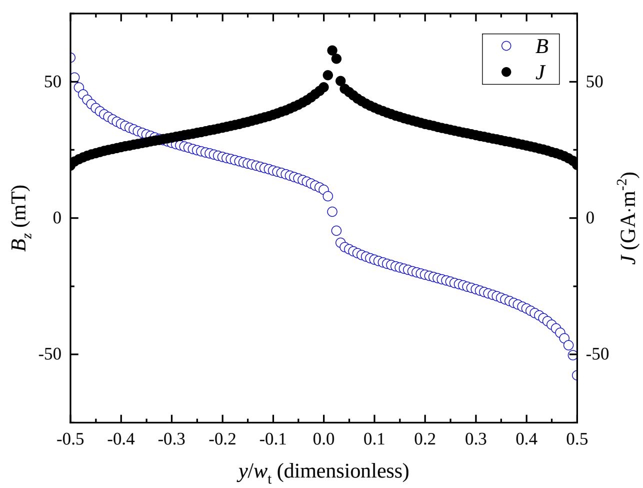

Fig. 3. The spatial distribution of the magnetic field in the z-direction and the critical current density within the tape, where the width of the component JJs w_{s} = 200 nm, and the applied field B_{app} = 1 mT. Note that the local magnetic field in the tape is much larger than the applied field.

where a_0 and a_1 are constants given by $a_0 = 0.357$ and $a_1 = 0.656$ when we fit to the peaks of the data in Fig. 1 and $a_0 = 0.181$ and $a_1 = 0.759$ when we fit to field-averaged values. In both cases, aspect ratios $0.05 < L/w_{\mathrm{s}} < 5$ are used where L is the length of the superconducting electrodes. Equation (9) can be used to reduce the number of free parameters in (7).

IV. Self Field Calculations

Self-field calculations for local spatially varying $J_{\mathrm{c}}(B)$ have been made by a number of authors for thin strips [7]–[10] using for example the Kim model [11].

We have used the expression for the magnetic vector potential of a thin strip in terms of the current distribution [7], to find the magnetic field where

$$B_z(y) = B_{\text{app}} + \frac{\mu_0 t}{2\pi}\int_{-w_t/2}^{w_t/2} \frac{J_c(B_z(u))}{y-u}\mathrm{d}u, \tag{10}$$

w_t is the width of the tape, t its thickness and B_{app} is the applied field. This gives a width-independent solution for $B_z(y)$ where the self-field is linear with thickness. Because our relation for the field dependence of $J_c(B)$ is strongly peaked around $B = 0$ (see (7)), unlike the Kim model, we cannot assume that the gradient in the magnetic field is small everywhere and have to include higher-order terms to find accurate solutions. The second derivative terms are most important where the local field is zero and the current density at its peak value. We have made a Taylor expansion to second order in the derivative of the current to evaluate the integral at each grid point from $y_i - \Delta y/2$ to $y_i + \Delta y/2$:

$$\begin{aligned}\frac{\pi}{\mu_0 b}\left(B(y_j) - B_{\text{app}}\right) \approx \sum_i \ln\left(\frac{y_i + \frac{\Delta y}{2} - y_j}{y_i - \frac{\Delta y}{2} - y_j}\right) J(y_i) \\ + \left(\Delta y - (y_i - y_j)\ln\left(\frac{y_i + \frac{\Delta y}{2} - y_j}{y_i - \frac{\Delta y}{2} - y_j}\right)\right) \left.\frac{\mathrm{d}J}{\mathrm{d}y}\right|_{y_i} + \\ \left((y_i - y_j)^2 \ln\left(\frac{y_i + \frac{\Delta y}{2} - y_j}{y_i - \frac{\Delta y}{2} - y_j}\right) - (y_i - y_j)\,\Delta y\right) \left.\frac{\mathrm{d}^2 J}{\mathrm{d}y^2}\right|_{y_i}.\end{aligned} \tag{11}$$

When the grid spacing $\Delta y \ll |y_i - y_j|$, this reduces to the expected $\sum J/(y_i - y_j)$, but for the points $j-1, j, j+1$ the additional contributions are not small. Including these gradient terms from the point of interest and its nearest neighbours gives:

$$\begin{aligned}\frac{\pi B(y_j)}{\mu_0 b \Delta y} = \sum_{i \neq j} \frac{J(y_i)}{y_i - y_j} - \left.\frac{\mathrm{d}J}{\mathrm{d}y}\right|_{y_j} + (\ln(3) - 1) \\ \times \left(J(y_{j+1}) - J(y_{j-1}) - \left.\frac{\mathrm{d}J}{\mathrm{d}y}\right|_{y_{j+1}} - \left.\frac{\mathrm{d}J}{\mathrm{d}y}\right|_{y_{j-1}} \right. \\ \left. + \frac{1}{2}\left.\frac{\mathrm{d}^2 J}{\mathrm{d}y^2}\right|_{y_j+1} - \frac{1}{2}\left.\frac{\mathrm{d}^2 J}{\mathrm{d}y^2}\right|_{y_j-1}\right).\end{aligned} \tag{12}$$

Typically we used approximately 100 grid points across the strip. Equation (12) is then used with (7), where B is taken to be the local magnetic field, and they are solved iteratively to find the spatial variation of the critical current density across the strip and hence the total critical current of the tape. Similar field distributions have been found experimentally [12]–[16].

Next we find an estimate of the cross-over field by considering a thin cylindrical shell carrying a uniform current density flowing in the direction of the axis of the shell. From symmetry, the magnetic field is entirely circumferential and from Ampère's law, the volumetrically averaged magnetic field within the cylindrical shell itself B_{cyl} is given by $B_{\text{cyl}} w_{\text{shell}} = \mu_0 I/2$, where w_{shell} is the circumference of the shell. We can assume that at the cross-over field, the applied field is sufficiently large to rotate the net field everywhere throughout the shell into the direction of the applied field which gives the condition $B_{\text{app}} = B_{\text{cr}} = B_{\text{cyl}}$, and using $J = I/w_{\text{shell}} t$ leads to an expression for the cross-over field given by

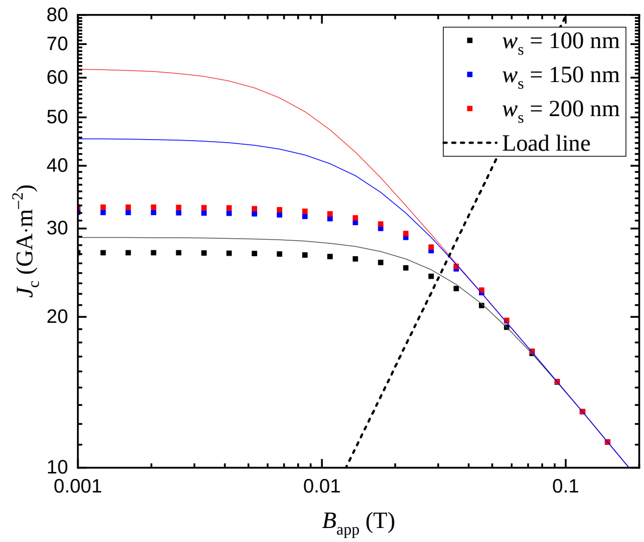

Fig. 4. The effect of self-field on $J_c(B)$ for a range of junction widths, w_s. The other parameters have been rescaled for each width to match the Fujikura in-field $J_c(B)$ data at 77 K from [24]. Lines show the local $J_c(B)$ relation from (7), points are the average of the J_c distribution with self-field. Also shown is the load line given by (13). At fields below the load line, the average J_c is not strongly dependent on the local J_c relation.

$$B_{\text{cr}} = \frac{\mu_0 J_c(B_{\text{app}} \leq B_{\text{cr}}) t}{2}. \tag{13}$$

In Fig. 3, the spatially varying field and current density are shown for the Fujikura fit-parameters with $w_s = 200\,\text{nm}$. The average magnitude of the field and the average of the current density are approximately related by (13) in Fig. 3 which demonstrates that the cross-over field can equally be considered the condition for the applied field to equal the average z-component of the self-field. In Fig. 4 we have varied w_s in (7) and calculated the equivalent current density as a function of the applied field. As shown in the figure, the cross-over field is broadly in agreement with (13) - only dependent on J_c and t and independent of w_s. Below the cross-over field, J_c is broadly constant.

Using the approximate power-law field dependence implicit in either (1) or (7) for J_c in magnetic fields above B_{cr}, we can find the thickness dependence of $J_c(0)$ in self-field. Consider two tapes of thickness t_1 and t_2 of identical quality so that in high magnetic fields J_c for the two tapes is the same. Using (13) and the power law for J_c gives the self-field values for the two tapes as

$$\frac{J_c^{t_2}(B_{\text{app}} = 0)}{J_c^{t_1}(B_{\text{app}} = 0)} = \left(\frac{t_1}{t_2}\right)^{\frac{c_1}{1+c_1}}, \tag{14}$$

which given that c_1 is typically 0.6, shows a strong thickness dependence. For example, if we double the thickness of a tape and retain the same J_c in high fields, we can expect the self-field J_c to decrease by $\sim 20\,\%$. A decrease in self-field J_c with thickness has been seen by many authors [17]–[22] (but not all [23]) and is often attributed to defects.

TABLE I
FIT PARAMETERS FOR EQUATION (7)

Parameter	Fujikura	SuNAM	THEVA
$\tilde{\beta}_{\mathrm{n}}$	0	0	0
T_{cn} (K)	1.27	1.27	1.27
$\tilde{m}_{\mathrm{n}}/\tilde{\Upsilon}_{\mathrm{n}}(0)$	4.56	4.56	4.56
d (nm)	3.28	2.96	3.72
w_{s} (nm)	100	108	67
c_1	0.56	0.57	0.56
t (µm)	2	1.5	3.5

V. Comparison to Experimental Results

In this paper, we have used the experimental data from Tsuchiya *et al.* [24], who have measured a number of different commercial REBCO tapes at 4.2 K and 77 K, as well as data on THEVA tapes from Gurnham *et al.* [25] at 77 K. First the free parameters for (7) were found by fitting the J_{c} above 0.5 T at both 4.2 K and 77 K. We imposed a minimum value of 0.56 on c_1, see Fig. 2. Good fits were only obtained with small $\tilde{\beta}_{\mathrm{n}}$, so we have set this to 0. The values of the parameters used are listed in Table I. The fit values for the normal state properties T_{cn} and $\tilde{m}_{\mathrm{n}}/\tilde{\Upsilon}_{\mathrm{n}}(0)$ from the Fujikura tape were fixed for the SuNAM tape, with the junction geometry parameters, d, w_{s} and c_1, kept free. For the THEVA data, we performed a fit including a self-field correction to the $B_{\mathrm{app}} = 0$ point to constrain the relation between d and w_{s} in the absence of temperature variation. Then using (7) to define J_{c} as a function of the local magnetic field, (12) was used to find J_{c} as a function of applied field with the self-field corrections included. As shown in Fig. 5 from the J_{c} at 4.2 K, the self-field correction reduces the currents measured at the low fields and increases the field at which there is a cross-over from the field independent regime for J_{c} to the power-law regime for J_{c}. We note that the uncertainties in the free parameters are relatively large because the crossover field is not precisely measured in the data. We have also plotted (13) and good agreement with the experimental cross-over field is demonstrated.

VI. Conclusion

We have completed an analysis of the critical current density of REBCO tapes in low applied magnetic fields: i) We have extended the high field expression for J_{c} to low applied fields and proposed a functional form that correctly crosses over to the self-field regime at low field (see (7)). This has value for computational parameterisation because it ensures that non-physical very high values of J_{c} are avoided and is particularly useful for characterisation of the properties of tapes for use in magnet design. ii) We have completed numerical calculations that provide the spatial variation of the current density and z-component of the magnetic field in thin REBCO tapes that are useful when the self-field is comparable to the applied field. We have provided a method, by including higher order terms, that can be used to self-consistently calculate the current density of a wide tape with self-field corrections. iii) By considering the properties of an infinitesimally thin cylindrical shell, we have found an expression, (13), for the cross-over

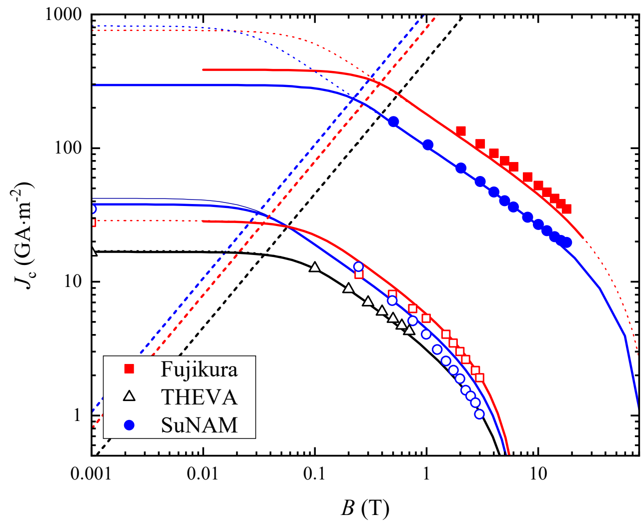

Fig. 5. J_{c} data at 4.2 K and 77 K for a Fujikura and a SuNAM tape [24], and at 77 K for a THEVA tape [25]. Open symbols are experimental data at 77 K and closed symbols are at 4.2 K. Solid lines are fits to the experimental data and dotted lines are the local $J_{\mathrm{c}}(B)$ input data used. Also shown are dashed lines for the cross-over fields given by (13).

field between low fields, where the self-field is larger than the applied field and high fields where the opposite holds. This cross-over field is important because the mechanism for dissipation changes completely from fluxons and anti-fluxons penetrating at opposite sides of the tape with fluxon-antifluxon annihilation above J_{c} at low fields, to fluxons entering one side of the tape, traversing the tape and leaving through the other side in high fields above the cross-over field. Different dissipative processes, along with a commensurately different mechanism for determining J_{c} below and above the crossover field provide a natural explanation for the well-know lack of correlation between J_{c} measured in zero applied field and J_{c} in high magnetic fields [26], [27]. This cross-over field expression is sufficiently simple to provide a means to determine from a single measurement of J_{c} in low fields whether it is above or below the cross-over field. The magnitude of the cross-over field also provides a useful minimum value for the local field when optimising the performance of high field superconducting systems using tapes. We also note that if a film with good uniform pinning properties is made thicker, (7) will lead to a significant reduction in J_{c} measured in zero applied field because of self-field effects. iv) We have fitted data in low fields at two different temperatures that self-consistently included the spatial distribution of J_{c} and demonstrated that we can find relevant free parameters and self-consistent solutions for the macroscopic J_{c} that agree with data from the literature.

Acknowledgment

The authors would like to thank: S Lishman, J Greenwood and M Raine for their help. The data are available at http://dx.doi.org/10.15128/r1d504rk36k and associated materials can be found at Durham Research Online: http://dro.dur.ac.uk/. The code is available on request from DPH.

REFERENCES

[1] A. I. Blair and D. P. Hampshire, "The critical current density of SNS Josephson junctions and polycrystalline superconductors in high magnetic fields," 2021, arXiv:2110.02053.

[2] H. J. Fink, "Supercurrents through superconducting-normal-superconducting proximity layers. I. Analytic solution," *Phys. Rev. B*, vol. 14, no. 3, pp. 1028–1038, Aug. 1976.

[3] J. R. Clem, "Josephson junctions in thin and narrow rectangular superconducting strips," *Phys. Rev. B*, vol. 81, no. 14, Apr. 2010, Art. no. 144515.

[4] D. R. Tilley and J. Tilley, *Superfluidity and Superconductivity*, 3rd ed. Bristol, UK: IOP, 1990, ch. 8, sec. 4, pp. 303–312.

[5] P. Branch, K. Osamura, and D. Hampshire, "Weak emergence in the angular dependence of the critical current density of the high temperature superconductor coated conductor REBCO," *Supercond. Sci. Technol.*, vol. 33, no. 10, Sep. 2020, Art. no. 104006.

[6] C. J. Gorter and H. Casimir, "On supraconductivity I," *Physica*, vol. 1, pp. 306–320, 1934.

[7] A. A. Babaei Brojeny and J. R. Clem, "Self-field effects upon the critical current density of flat superconducting strips," *Supercond. Sci. Technol.*, vol. 18, no. 6, pp. 888–895, May 2005.

[8] L. Rostila, J. Lehtonen, and R. Mikkonen, "Self-field reduces critical current density in thick YBCO layers," *Physica C*, vol. 451, no. 1, pp. 66–70, Jan. 2007.

[9] A. Sanchez, C. Navau, N. Del-Valle, D.-X. Chen, and J. R. Clem, "Self-fields in thin superconducting tapes: Implications for the thickness effect in coated conductors," *Appl. Phys. Lett.*, vol. 96, no. 7, Feb. 2010, Art. no. 072510.

[10] Ö. Polat, J. W. Sinclair, Y. L. Zuev, J. R. Thompson, D. K. Christen, S. W. Cook, D. Kumar, Y. Chen, and V. Selvamanickam, "Thickness dependence of magnetic relaxation and E–J characteristics in superconducting (Gd-Y)-Ba-Cu-O films with strong vortex pinning," *Phys. Rev. B*, vol. 84, Jul. 2011, Art. no. 024519.

[11] Y. B. Kim, C. F. Hempstead, and A. R. Strnad, "Magnetization and critical supercurrents," *Phys. Rev.*, vol. 129, no. 2, pp. 528–535, Jan. 1963.

[12] X.-F. Li, A. B. Yahia, G. Majkic, M. Kochat, S. Kar, and V. Selvamanickam, "Reel-to-reel critical current measurement of REBCO coated conductors," *IEEE Trans. Appl. Supercond.*, vol. 27, no. 4, Jun. 2017, Art. no. 3800205.

[13] E. F. Talantsev, N. M. Strickland, S. C. Wimbush, and W. P. Crump, "The onset of dissipation in high-temperature superconductors: Self-field experiments," *AIP Adv.*, vol. 7, no. 12, Dec. 2017, Art. no. 125230.

[14] E. F. Talantsev, W. P. Crump, and J. L. Tallon, "Universal scaling of the self-field critical current in superconductors: from sub-nanometre to millimetre size," *Sci. Rep.*, vol. 7, Aug. 2017, Art. no. 10010.

[15] E. F. Talantsev, N. M. Strickland, S. C. Wimbush, J. Brooks, A. E. Pantoja, R. A. Badcock, J. G. Storey, and J. L. Tallon, "The onset of dissipation in high-temperature superconductors: magnetic hysteresis and field dependence," *Sci. Rep.*, vol. 8, Sep. 2018, Art. no. 14463.

[16] N. Chikumoto, S. Yamaguchi, and O. Shyshkin, "Transport current distribution in soldered joint of BSCCO and REBCO tapes," *J. Phys.: Conf. Ser.*, vol. 1559, Jun. 2020, Art. no. 012069.

[17] S. R. Foltyn, Q. X. Jia, P. N. Arendt, L. Kinder, Y. Fan, and J. F. Smith, "Relationship between film thickness and the critical current of $YBa_2Cu_3O_{7-\delta}$-coated conductors," *Applied Physics Letters*, vol. 75, no. 23, pp. 3692–3694, Dec. 1999.

[18] S. I. Kim, A. Gurevich, X. Song, X. Li, W. Zhang, T. Kodenkandath, M. W. Rupich, T. G. Holesinger, and D. C. Larbalestier, "Mechanisms of weak thickness dependence of the critical current density in strong-pinning *ex situ* metal–organic-deposition-route $YBa_2Cu_3O_{7-x}$ coated conductors," *Supercond. Sci. Technol.*, vol. 19, no. 9, pp. 968–979, Aug. 2006.

[19] H. Zhou, B. Maiorov, S. A. Baily, P. C. Dowden, J. A. Kennison, L. Stan, T. G. Holesinger, Q. X. Jia, S. R. Foltyn, and L. Civale, "Thickness dependence of critical current density in $YBa_2Cu_3O_{7-\delta}$ films with $BaZrO_3$ and Y_2O_3 addition," *Supercond. Sci. Technol.*, vol. 22, no. 8, Jul. 2009, Art. no. 085013.

[20] H.-S. Ha, J.-H. Lee, R.-K. Ko, H.-S. Kim, H.-K. Kim, S.-H. Moon, C. Park, D.-J. Youm, and S.-S. Oh, "Thick SmBCO/IBAD-MgO coated conductor for high current carrying power applications," *IEEE Trans. Appl. Supercond.*, vol. 20, no. 3, pp. 1545–1548, May 2010.

[21] M. Igarashi, K. Kakimoto, T. Hayashida, Y. Hanada, S. Fujita, K. Morita, N. Nakamura, S. Hanyu, Y. Sutoh, H. Kutami, Y. Iijima, and T. Saitoh, "High-speed deposition of RE123 film with large current capacity by hot-wall type PLD system," *Physica C*, vol. 470, no. 20, pp. 1230–1233, Nov. 2010.

[22] L. Liu, Y. Li, G. Xiao, and X. Wu, "Fabrication of thick REBCO–coated conductors with high performance on metal tapes by pulsed laser deposition process," *J. Supercond. Nov. Magn.*, vol. 28, no. 2, pp. 403–406, Feb. 2015.

[23] M. Dürrschnabel, Z. Aabdin, M. Bauer, R. Semerad, W. Prusseit, and O. Eibl, "$DyBa_2Cu_3O_{7-x}$ superconducting coated conductors with critical currents exceeding 1000 A cm^{-1}," *Supercond. Sci. Technol.*, vol. 25, no. 10, Aug. 2012, Art. no. 105007.

[24] K. Tsuchiya, A. Kikuchi, A. Terashima, K. Suzuki, K. Norimoto, M. Tawada, M. Masuzawa, N. Ohuchi, X. Wang, Y. Iijima, T. Takao, S. Fujita, M. Daibo, and Y. Iijima, "Critical current characterization of commercial REBCO coated conductors at 4.2 and 77 K," *IEEE Trans. Appl. Supercond.*, vol. 27, no. 4, Jun. 2017, Art. no. 6600205.

[25] C. W. A. Gurnham, V. Große, and D. P. Hampshire, "Angular J_c measurements at 77 K in-field, on an ISD REBCO coated conductor using a straightforward mechanical scribing technique to reduce tape width," *J. Phys.: Conf. Ser.*, vol. 1559, Jun. 2020, Art. no. 012036.

[26] V. Selvamanickam, A. Xu, Y. Liu, N. D. Khatri, C. Lei, Y. Chen, E. Galstyan, and G. Majkic, "Correlation between in-field critical currents in Zr-added $(Gd, Y)Ba_2Cu_3O_x$ superconducting tapes at 30 and 77 K," *Supercond. Sci. Technol.*, vol. 27, no. 5, Mar. 2014, Art. no. 055010.

[27] G. Majkic, R. Pratap, E. Galstyan, and V. Selvamanickam, "Correlation of in-field performance of thick REBCO films between 0-14 T and 4.2–77 K," *IEEE Trans. Appl. Supercond.*, vol. 29, no. 5, Aug. 2019, Art. no. 6602005.